Molecular and Cellular Endocrinology 551 (2022) 111663

Contents lists available at ScienceDirect

Molecular and Cellular Endocrinology

journal homepage: www.elsevier.com/locate/mce

Mechanisms by which smoothelin-like protein 1 reverses insulin resistance in myotubules and mice

Istvan Tamas [a], Evelin Major [a], Daniel Horvath [a], Ilka Keller [a], Adam Ungvari [a], Timothy A. Haystead [b], Justin A. MacDonald [c], Beata Lontay [a,*]

[a] Department of Medical Chemistry, Faculty of Medicine, University of Debrecen, Debrecen, Hungary
[b] Duke University School of Medicine, Department of Pharmacology and Cancer Biology, Durham, NC, USA
[c] Department of Biochemistry and Molecular Biology, Cumming School of Medicine, University of Calgary, Calgary, AB, Canada

ARTICLE INFO

Keywords:
Insulin resistance
Skeletal muscle metabolism
Pregnancy
Insulin signaling
Insulin receptor substrate-1
Phosphorylation

ABSTRACT

Insulin resistance (InR) is manifested in skeletal muscle by decreased insulin-stimulated glucose uptake due to impaired insulin signaling and multiple post-receptor intracellular defects. Chronic glucose-induced insulin resistance leads to the activation of Ser/Thr kinases and elevated phosphorylation of insulin receptor substrate 1 (IRS1) on Ser residues. Phosphorylation of IRS1 triggers the dissociation of IRS1 and its downstream effector, phosphatidylinositol 3-kinase. In the present study, we provide evidence for the insulin-sensitizing role of smoothelin-like protein 1 (SMTNL1) that is a ligand-dependent co-regulator of steroid receptors, predominantly the progesterone receptor. SMTNL1 was transiently overexpressed in insulin-resistant C2C12 myotubes. A proteome profiler array revealed that mTOR and Ser/Thr kinases were SMTNL1-dependent signaling pathways. In the presence of progesterone, overexpression was coupled to decreased Ser phosphorylation of IRS1 at Ser307, Ser318, and Ser612 residues. SMTNL1 also induced the expression and activity of the p85 subunit of PI3K. SMTNL1 regulated the expression of PKCε, which phosphorylates IRS1 at Ser318 residue. SMTNL1 also regulated ERK1/2 and JNK, which phosphorylate IRS1 at Ser612 and Ser307, respectively. Real-time metabolic measurements of oxygen consumption rate and extracellular acidification rate revealed that SMTNL1 improved glycolysis and promoted the utilization of alternative carbon fuels. SMTNL1 also rescued the mitochondrial respiration defect induced by chronic insulin exposure. Collectively, SMTNL1 plays a crucial role in maintaining the physiological ratio of Tyr/Ser IRS1 phosphorylation and attenuates the insulin-signaling cascade that contributes to impaired glucose disposal, which makes it a potential therapeutic target for improving InR.

Highlights.

- SMTNL1 promotes insulin sensitivity in insulin-resistant skeletal muscle
- SMTNL1 regulates the expression of novel PKCε that contributes to the phosphorylation of IRS1 at Ser318 residue
- SMTNL1 regulates ERK1/2 activity therefore IRS1 Ser612 phosphorylation
- SMTNL1 hampers JNK1 activity to regulate IRS1 Ser307 phosphorylation
- SMTNL1 promotes glucose uptake via activation of Akt activity and by inducing GLUT4 expression

1. Introduction

Insulin resistance syndrome affects about 24% of adults older than 20 years and is manifested as a variety of disorders, including glucose tolerance impairment, type 2 diabetes, obesity, and reproductive disorders (Meigs, 2003). Insulin resistance (InR) is characterized by decreased cellular responsiveness to insulin signaling in insulin-dependent tissues, such as skeletal muscle, liver, and adipose tissue. When muscle, fat, and liver cells become resistant to the action of insulin, pancreatic β-cells respond by pumping increased amounts of insulin into the circulation to maintain homeostatic control of glucose level (Boucher et al., 2014).

Skeletal muscle (SKM) is the major site of ingested glucose disposal in normal glucose tolerant individuals (Abdul-Ghani and DeFronzo, 2009). While the liver takes up approximately one-third of post-prandial

* Corresponding author. Department of Medical Chemistry, Faculty of Medicine University of Debrecen, H-4032, Debrecen, Egyetem tér 1, Hungary.
E-mail address: lontay@med.unideb.hu (B. Lontay).

https://doi.org/10.1016/j.mce.2022.111663
Received 29 September 2021; Received in revised form 27 April 2022; Accepted 27 April 2022
Available online 1 May 2022

Abbreviations

2-DG	2-deoxy-D-glucose
ANOVA	analysis of variance
DMEM	Dulbecco's modified Eagle's medium
ECAR	extracellular acidification rate
ERK1/2	extracellular signal-regulated kinase
FT-SMTNL1	N-terminal FLAG tag SMTNL1
GDM	gestational diabetes mellitus
Glut4	glucose transporter 4
InR	insulin resistance
IR	insulin receptor
IRS1	insulin receptor substrate
JNK	c-Jun N-terminal kinase
MPA	medroxyprogesterone-17-acetate
OCR	oxygen consumption rate
PI3K	phosphatidylinositol 3-kinase
PKA	protein kinase A
PKCε	protein kinase epsilon
PKCζ	protein kinase C zeta
PKG	protein kinase A
PR	progesterone receptor
RIPA	radioimmunoprecipitation assay buffer
SKM	skeletal muscle
SMTNL1	smoothelin-like protein 1

glucose in the bloodstream, the remainder is taken up by peripheral tissues, primarily by SKM via an insulin-dependent mechanism. The binding of insulin to the insulin receptor (IR) initiates a signaling cascade that results in the translocation of the insulin-sensitive glucose transporter protein 4 (GLUT4) to the plasma membrane to facilitate the transport of glucose into the cell. IR activation upon insulin binding results in phosphorylation of the insulin receptor substrate 1 (IRS1) protein, that in turn docks and activates phosphatidylinositol 3-kinase (PI3K) that goes under conformational changes in its catalytic domain, which in turn results in kinase activation. This is followed by the PI3K-mediated phosphorylation of membrane bound PIP2 to generate PIP3. PIP3 then binds to the PH domain of Akt, thereby anchoring it to the plasma membrane to transduce the insulin signal to a serine/threonine (Ser/Thr) protein kinase, Akt/protein kinase B (Boucher et al., 2014). Upon membrane recruitment of Akt, it is phosphorylated and activated in its kinase domain at Thr308 and for substrate selectivity and activity enhancement at Ser473 by phosphoinositide-dependent protein kinase 1 and mTORC2, respectively (Beg et al., 2017). Akt phosphorylates and inhibits AS160, removing its inhibition of Rab proteins. Ultimately, Akt can promotes the translocation of GLUT4-containing vesicles to the plasma membrane to mediate insulin-stimulated glucose transport in SKM (Kupriyanova and Kandror, 1999) (Kohn et al., 1996).

InR is manifested in SKM by decreased insulin-stimulated glucose uptake resulting from impaired insulin signaling and multiple intracellular post-receptor defects, including impaired glucose transport and conversion to glucose-6-phosphate, reduced glucose oxidation, and attenuated glycogenesis. Insulin action is inhibited by enhanced Ser/Thr phosphorylation of either the receptor or its downstream effectors; this increased phosphorylation affects their mutual interactions and reduces the relative contribution of each of the elements in this signaling cascade, resulting in decreased IRS activity or its ability to recruit substrate proteins and thus to propagate insulin signaling (Mlinar et al., 2007). Cytokines, and hyperinsulinemia initiate phosphorylation by enhancing Ser phosphorylation and reducing Tyr phosphorylation of IRS1, which leads to decreased glucose uptake and insulin resistance (Boucher et al., 2014).

One potential regulator of insulin resistance in SKM is the smoothelin-like 1 protein (SMTNL1). SMTNL1 is a target of protein kinase A and G (PKA/PKG) and is expressed in smooth and skeletal muscles (Borman et al., 2004) as well as steroid hormone-sensitive tissues (Bodoor et al., 2011; Wooldridge et al., 2008). It has a dual function: on one hand, it regulates muscle contraction and the cytoskeletal elements of various cells through the inhibition of the activity of myosin phosphatase holoenzyme. Through this regulation, it enhances the phosphorylation of the regulatory 20 kDa light chain of myosin (Bodoor et al., 2011; Lontay et al., 2010). On the other hand, upon phosphorylation at Ser301 by PKG/PKA, SMTNL1 translocates to the nucleus where it functions as a transcriptional regulator of steroid receptors, predominantly the progesterone receptor (PR). (Bodoor et al., 2011; Lontay et al., 2010). In a progesterone-dependent manner, SMTNL1 can regulate the gene expression of dozens of metabolic enzymes, cytoskeletal elements, steroid receptors, and cytokines (Bodoor et al., 2011). In addition, SMTNL1 promotes adaptive responses to pregnancy in mice by reprogramming the metabolic and contractile character of SKM to increase power/strength and the glycogen content required for managing weight gain during fetal development (Lontay et al., 2015). Pregnancy promotes muscle fiber-type changes from an oxidative to a glycolytic isoform in SKM. This phenomenon is regulated through the interaction between SMTNL1 and PR, which alters the expression of contractile and metabolic proteins (Lontay et al., 2015).

The current study aimed to explore the detailed molecular impact of SMTNL1 on InR development in SKM during pregnancy using *Smtnl1* knockout (KO) mice and insulin-resistant differentiated C2C12 myotubes. We hypothesized that SMTNL1 modulates insulin signaling pathways by regulating the expression of upstream modulators of Ser/Thr kinases responsible for the phosphorylation of IRS-1 and resulting in the dissociation of PI3K and the inactivation of the IRS-1/PI3K/Akt/mTOR pathway.

2. Material and methods

2.1. Materials

All chemicals were obtained from Sigma-Aldrich (St. Louis, MO, USA) unless indicated otherwise. Microcystin-LR was produced and purified as described previously (Mathe et al., 2009).

2.2. Antibodies

All antibodies are listed in Table S1.

2.3. Cell maintenance, differentiation, and insulin resistance model

The C2C12 mouse myoblast cell line (Sigma-Aldrich) was cultured in low-glucose (5.5 mM) DMEM supplemented with 2 mM L-glutamine and 10% (v/v) FBS in a 5% CO_2-humidified atmosphere at 37 °C. Cells were grown in collagen-coated petri dishes for differentiation (VWR West Chester, PA, USA) and maintained in differentiation medium (5.5 mM DMEM without phenol red, supplemented with 2 mM L-glutamine and 2% (v/v) horse serum) for 5 days (Fig. S1). Cells were lysed in radioimmunoprecipitation assay (RIPA) buffer (25 mM Tris-HCl pH 7.6, 150 mM NaCl, 0.25% (m/v) sodium deoxycholate, 1% (v/v) NP-40, 0.1% (m/v) sodium dodecyl sulphate) containing protease and phosphatase inhibitors (1 mM NaF, 1 mM $Na_4P_2O_7$, 1 mM β-glycerol-phosphate, 1 mM Na_3VO_4) and 1 μM of microcystin-LR.

For the InR treatment, high glucose (HG, 25 mM glucose) DMEM without phenol red was supplemented with 2 mM L-glutamine, 2% horse

serum, and 100 nM of insulin (chronic insulin). The low glucose (LG, 5.5 mM glucose) DMEM without phenol red was supplemented with 2 mM L-glutamine, 2% (v/v) horse serum, and 50 pM of insulin and 10 nM of medroxyprogesterone-17-acetate (MPA) was added as described in Fig. S1. For Western-blotting, Proteome Profiler, and PI3K activity experiments the media was changed to serum and hormone-free DMEM medium for 5 h and cells were treated again for 30 min with 100 nM of insulin (acute insulin) before harvesting. Samples were prepared for the PI3K assay according to the supplementary protocol section for PI3K activity measurement. Proteins were solubilized as described before (Lontay et al., 2010). Protein concentrations were determined as described before (Sipos et al., 2017) (Fig. S1.).

2.4. Transient transfections

The full-length mouse SMTNL1 construct (pcDNA-3.1 expression vector) with N-terminal FLAG tag, referred to as FT-SMTNL1, and the empty pcDNA-3.1 plasmid as a transfection control, referred to as empty vector/control, were overexpressed in C2C12 cells on day 0 of the full-length protocol using GeneJuice Transfection Reagent (Novagen, Merck Millipore, Darmstadt, Germany).

2.5. Western blotting

Western blot analysis was conducted as described before (Sipos et al., 2017). Briefly, proteins were separated on Bio-Rad 4–20% Criterion TGX Precast Midi protein gels. Antibody binding was detected using enhanced chemiluminescence (Advansta WesternBright ECL, San Jose, CA, USA) and visualized using the Bio-Rad ChemiDoc Touch imaging system. Densitometric analysis was performed with Bio-Rad ImageLab 6.0 software. Membrane stripping was also applied with heat and detergent. Shortly, membranes were incubated in Stripping buffer [0.5 M Tris-HCl pH 6.8; 10% SDS, β-mercaptoethanol] at 50 °C for 30 min in a Thermo-Shaker (Biosan) and were washed 6 times for 5 min with 1x TBST and reblocked with 5% BSA/TBST at RT for 1 h and reprobed as described above.

2.6. Proteome profiler analysis

Phosphorylation levels of various proteins were analyzed with a R&D Systems Proteome Profiler Human Phospho-Kinase Array kit (Minneapolis, MN, USA). After the previously described treatments, cells were harvested and 200 μg of protein was used for each experiment, according to the manufacturer's instructions. Dot intensities were analyzed with ImageJ software (NIH, Bethesda, MD, USA) and normalized to control dots on each membrane.

2.7. PI3K activity measurement

PI3K activity was measured with an ELISA kit (PI3-Kinase Activity ELISA, Pico, Echelon Biosciences Inc., Salt Lake City, UT, USA) following the manufacturer's protocol. Absorbance was measured at 450 nm (Multiskan GO, Thermo Scientific). Immunoprecipitation was conducted with the p85 subunit antibody (Merck Millipore) to validate the input. Liberated phosphatidylinositol (3,4,5)-trisphosphate (PIP_3) values were normalized to the PI3K expression levels.

2.8. Seahorse XF96 measurements

For the metabolic measurements we altered the original differentiation/treatment protocol (Fig. S1.). After transfection, cells were plated, and 24 h after transfection, were treated for 72 h as described in 2.3. Cells were seeded in small petri dishes, to confirm the effectivity of transfection. After the 72 h, myoblast cells were washed, and metabolic measurements were made on Agilent Seahorse XF (ASX) 96 plates using ASX assay-medium with 5.5 mM glucose. Etomoxir (50 μM), which is an inhibitor of fatty acid oxidation (FAO) was added. Oligomycin (2 μM) was applied to inhibit ATP synthesis and distinguish between the O_2 consumption devoted to ATP synthesis. FCCP (4 μM, carbonyl cyanide p-trifluormethoxyphenylhydrazone) was used as a mobile ion carrier to calculate the respiratory capacity of cells. Antimycin A (10 μM) was applied as the inhibitor of complex III to shut down electron transport chain function, revealing the non-mitochondrial respiration. Finally, 100 mM 2-deoxy-D-glucose (2-DG) was added; 2-DG is a glucose analog that inhibits glycolysis through competitive binding to glucose hexokinase to confirm ECAR due to glycolysis. Five measurement points were taken at baseline and after each injection event. After the measurements, cells were solubilized in 1N NaOH and protein content was determined by BCA assay.

2.9. Glucose uptake assay

2-NBDG (2-(*N*-(7-Nitrobenz-2-oxa-1,3-diazol-4-yl)Amino)-2-Deoxyglucose) uptake measurements were carried out as described previously, shortly. C2C12 cells were cultured, differentiated and treated as described before (Section 2.3-4.). The myotubes were washed with PBS buffer and incubated in glucose free DMEM supplemented with 2% horse serum. 100 nM insulin was applied for 30 min and cells were incubated with glucose-free medium containing 100 μM 2-NBDG (SIGMA) for 120 min at 37 °C. Fluorescence was measured at an extinction of 485 nm and emission of 535 nm using a Tecan Spark Multimode microplate reader (Tecan Treading AG, Mannedorf, Germany), and negative and blank controls as well as standard curve were also sat up to quantify glucose uptake. Cells were washed three-times and were solubilized in 0.1 M KH_2PO_4 pH 11.0 to determine protein concentration. Fluorescent data in pmol were related to 1 mg of proteins in each case and presented as fold induction.

2.10. Statistical analysis

Post hoc testing for two-way ANOVA was determined by Tukey's test and Sidak's test. The mouse tissue sample data were analyzed with one-way ANOVA and Dunnett's *post hoc* test. Parametric tests were used when normalized values were normally distributed. GraphPad software was used for all analyses. The data are presented as mean ± SEM; n is the number of independently performed experiments or animals. $P < 0.05$ was considered statistically significant.

3. Results

3.1. SMTNL1 influences insulin signaling, cell cycle, and apoptosis in insulin resistant C2C12 cells

The mouse myoblast cell line, C2C12, is a widely-used model for the *in vitro* examination of metabolic diseases, such as insulin resistance (Wong et al., 2020). InR was induced with chronic insulin treatment and 10 nM MPA (synthetic progesterone) with or without the overexpression of Flag-tag-SMTNL1 (FT-SMTNL1) in C2C12 myotubes (Fig. S1.). The overexpression of FT-SMTNL1 and differentiation was verified by high content screening analysis (Fig. S2). Protein arrays were used to monitor the phosphorylation and activity status of Tyr and Ser/Thr kinases and receptors, transcription factors, and other elements of insulin signaling (Fig. 1). Data were compared to control samples under conditions of low glucose (Figs. 1 and S3). Two-fold increases in phosphorylation levels of transcription factors, including STAT5a and b, were observed in cells overexpressing SMTNL1; however, the phosphorylation levels of STAT2 and 6, CREB, and c-Jun were unaffected (Fig. S3B). Regarding cell cycle regulation, only p53 Ser46 phosphorylation was increased in the InR cells overexpressing FT-SMTNL1 (Fig. S3A). Pyk2 non-receptor tyrosine kinase and PDGF receptor tyrosine kinase phosphorylation increased after MPA treatment and in combination with SMTNL1 overexpression in InR cells (Figs. S3C and S3F). Several important Ser/Thr kinases were

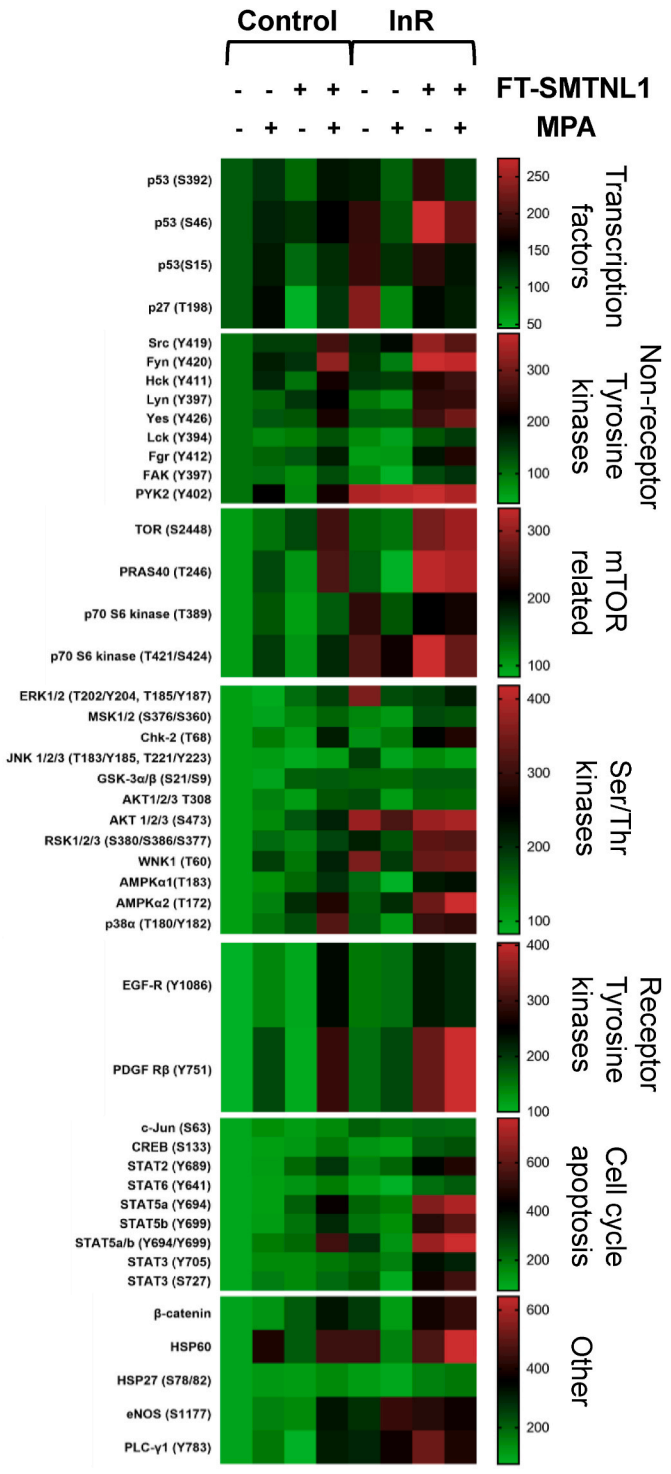

Fig. 1. Proteome profiler analysis of transfected and treated C2C12 cell lysates. A heatmap of various protein phosphorylation levels is shown. Color coding for the heatmap: red indicates more phosphorylated, while green indicates less phosphorylated protein levels. 200 μg of protein was used for the A and B part of membrane. The spot intensities were analyzed using ImageJ software and normalized to the control spots on each membrane.

elevated in response to induction of InR and were further increased by SMTNL1 overexpression (Fig. S3D). Phosphorylation of Thr172 in APMKα2 and Ser473 in Akt1/2/3 were increased by SMTNL1 overexpression in InR cells. In addition, phosphorylation of mTOR Ser2448 (Fig. S3E), c-Jun N-terminal kinase (JNK1/2/3) Thr183, and extracellular signal-regulated kinase (ERK1/2) Thr202 was increased (Fig. S3D); however, phosphorylation of p38, Chk2, and MSK1/2 did not change (Fig. S3D). These results indicate that SMTNL1 modulates critical signal transduction elements involved in insulin signaling and its downstream regulatory effects.

3.2. SMTNL1 overexpression decreases phosphorylation of ser residues of IRS1 in differentiated C2C12 insulin-resistant cells

To verify the protein phosphorylation results from the Proteome Profiler analysis and to elucidate the molecular mechanism underlying the effect of SMTNL1, we analyzed site-specific phosphorylations of IRS1 in InR C2C12 cells by Western blotting (Fig. 2). Moreover, to gain an understanding of the transcriptional changes induced by FT-SMTNL1 overexpression, we also looked at the levels of IRS1 and other signaling proteins (Figs. S5 and S6). Chronic insulin treatment significantly decreased IRS1 expression (Fig. 2E). However, IRS1 Ser307 (Fig. 2A), Ser318 (Fig. 2B), and Ser612 (Fig. 2C) phosphorylations were significantly elevated in InR cells and treatment with MPA had no effects. Ser phosphorylation levels were significantly lower in cells overexpressing FT-SMTNL1 in the presence of MPA in all cases (Fig. 2A–C). In contrast, IRS1 Ser1101 phosphorylation decreased in InR with or without progesterone (Fig. 2D), and the overexpression of SMTNL1 significantly decreased the Ser1101 phosphorylation of IRS1 in the presence of high concentrations of insulin and progesterone (Fig. 2D). We confirmed these findings in WT and KO *Smtnl1* non-pregnant and pregnant mice where the IRS1 phosphorylation at Ser612 (Fig. S4B.) and Ser1101 (Fig. S4A.) was significantly increased in SKM of pregnant *Smtnl1*−/− mice. Since SMTNL1 acts to attenuate the phosphorylation of IRS1 on Ser307, Ser318, and Ser612 in the presence of its natural ligand, it suggest that SMTNL1 modulate the activity or gene expression of IRS-1-Ser/Thr kinases or phosphatase, while IRS1 Ser1101 regulation is a ligand-independent process.

3.3. SMTNL1 promotes the activity of PI3K in insulin resistant C2C12 cells

To elucidate the effect of SMTNL1 on PI3K activity in insulin treatment, we determined the protein level of the p85 subunit of PI3K (Fig. 3A). Chronic insulin exposure significantly decreased p85 levels; however, FT-SMTNL1 overexpression increased p85 expression when compared to the empty vector transfection control. The PI3K enzyme activity, as determined by measuring the liberated PIP_3 product (Fig. 3B.), was not affected by either MPA exposure or FT-SMTNL1; however, PI3K activity was significantly increased in InR cells. Moreover, chronic insulin treatment in the presence of MPA induced higher PI3K activity compared to InR alone, and FT-SMTNL1 overexpression increased PI3K activity under conditions of InR. Collectively, these results demonstrate that SMTNL1 promotes PI3K activity in C2C12 myotubes by counteracting the decrease in PI3K protein levels triggered in response to chronic insulin exposure and by decreasing Ser phosphorylation of IRS1, which initiates the IRS1/PI3K complex.

3.4. Regulation of downstream effectors of insulin signaling by SMTNL1 in insulin resistance

The phosphorylation and activation of Akt/PKB in C2C12 myotubes was upregulated in the insulin-resistant state (Fig. 4A and B) and resulted in the propagation of downstream insulin signaling. Both Thr308 and Ser473 phosphorylation of Akt1 were stimulated by acute, 30 min insulin treatment, while MPA had no effect. Furthermore, the activity of Akt1 was increased in the InR model. FT-SMTNL1 overexpression did not influence the expression of Akt1 (Fig. S6B), but it drastically influenced the phosphorylation of Akt1 Ser473, but not Thr308, in InR myotubes, suggesting an insulin-sensitizing effect. These results are supported by interrogations of *Smtnl1* KO mice where Akt1 expression was unaffected in any experimental group (Fig. S4C.) but the

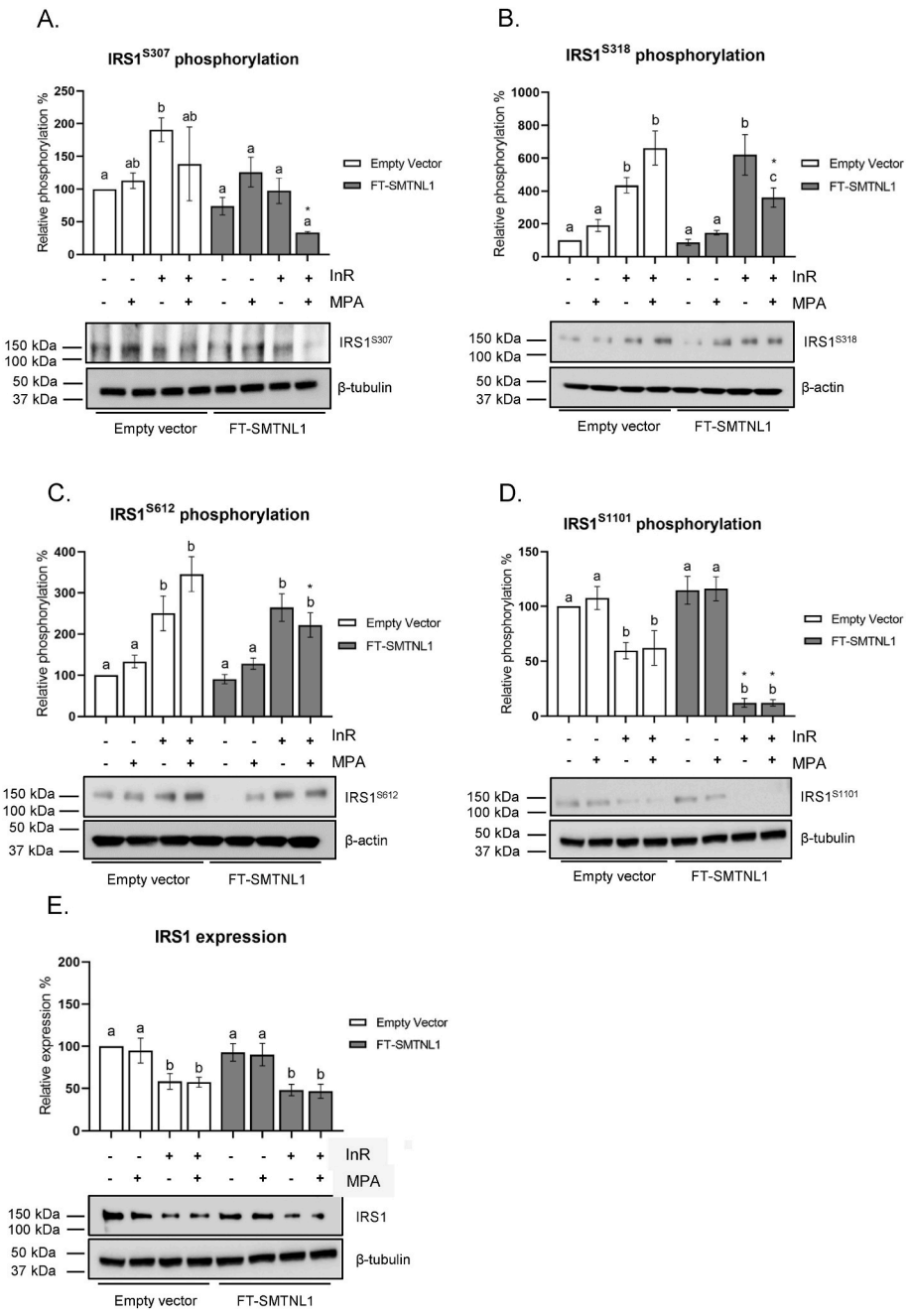

Fig. 2. Western-blot analysis of IRS1 expression and phosphorylation in insulin-resistant C2C12 myotubes. After differentiation and induction of insulin resistance, cells were harvested and prepared for Western blot analysis of $IRS1^{S307}$ **(A)**, $IRS1^{S318}$ **(B)**, $IRS1^{S612}$ **(C),** and $IRS1^{S1101}$ **(D)** phosphorylation and (E) IRS expression. The phosphorylation levels were normalized to non-phosphorylated protein which in turn was normalized to β-tubulin as an internal loading control. The effects of SMTNL1 vs. the empty vector-transfected cells were compared (Two-way ANOVA and Sidak's *post hoc* test, Mean ± SEM; n = 3; *, $p < 0.05$). The effects of various treatments were also compared (Two-way ANOVA and Tukey's *post hoc* test, Mean ± SEM; n = 3; $p < 0.05$; Different letters indicate significant differences between the groups compared).

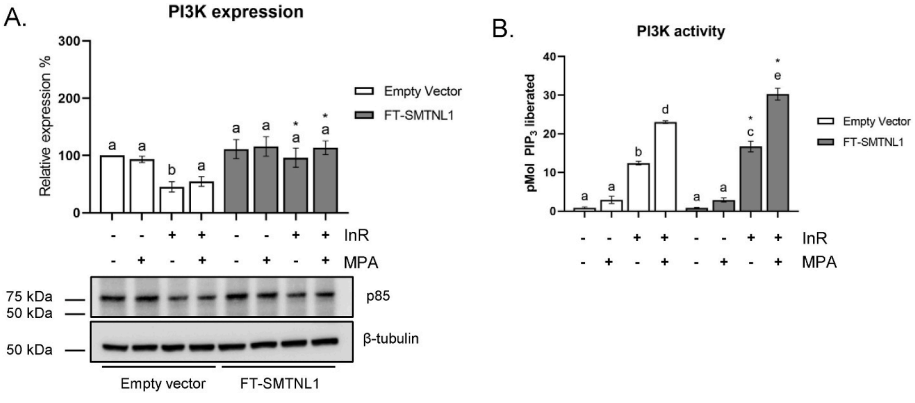

Fig. 3. SMTNL1 Promotes the activity of PI3K in insulin resistant C2C12 cells (A) Western blot analysis was conducted to determine the PI3K p85 subunit levels. Protein expression was normalized to the loading control. **(B)** PI3K activity was measured using a PI3K pico-ELISA kit. InR: insulin resistant; MPA: medroxyprogesterone-17-acetate. The effects of SMTNL1 vs. the empty vector-transfected cells were compared (Two-way ANOVA and Sidak's *post hoc* test, Mean ± SEM; n = 3; *, $p < 0.05$), and the effects of various treatments were compared (Two-way ANOVA and Tukey's *post hoc* test, Mean ± SEM; n = 3; $p < 0.05$; Different letters indicate significant differences between the groups compared).

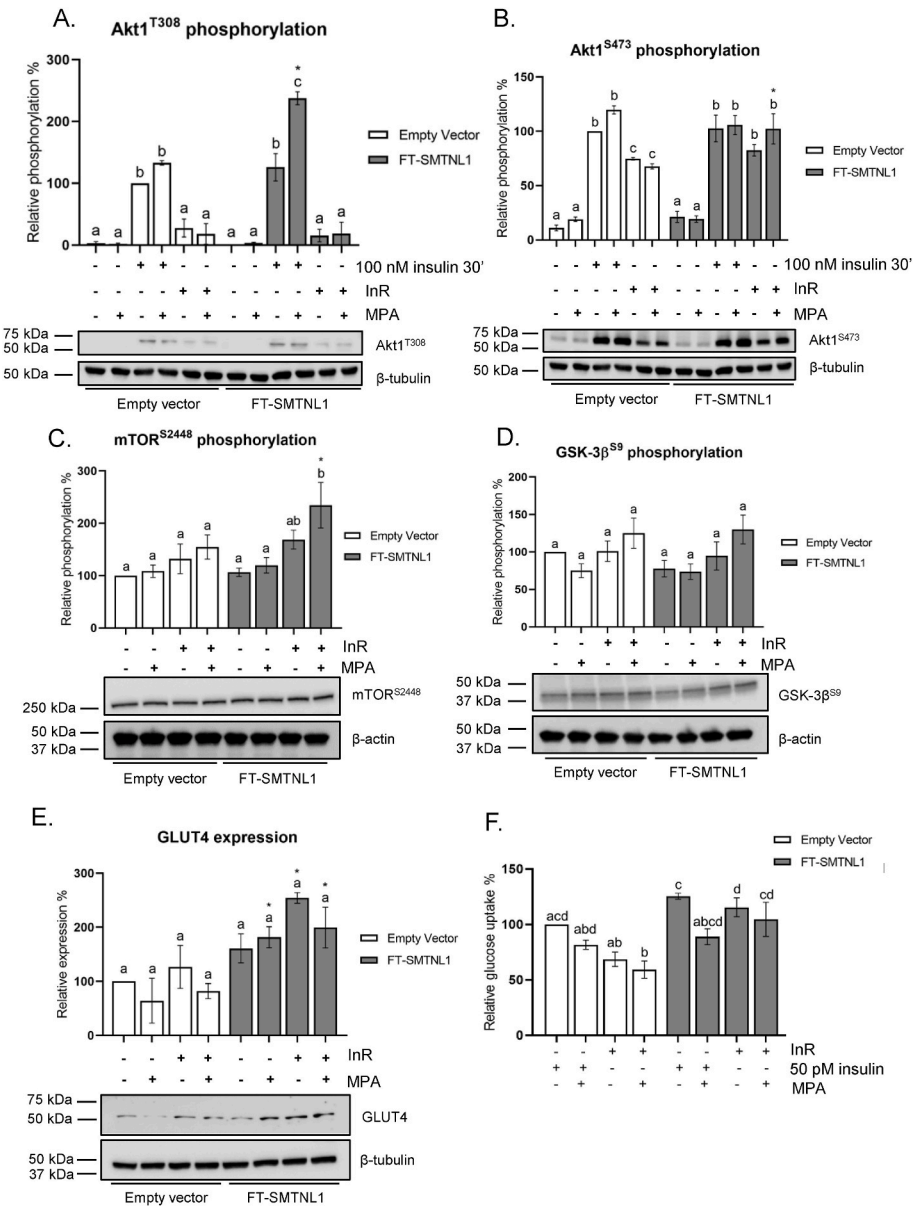

Fig. 4. Effects of SMTNL1 overexpression and insulin resistance on the insulin signaling pathway. For Akt1 phosphorylation **(A–B)** the same treatment method was used, except two more samples were introduced for each transfection. After the 72h of differentiation in physiological conditions, 100 nM of insulin were added to the cells for the final 30 min of treatment to assess if insulin resistance was present in the long-term treated cells. Samples were also collected to analyze other parts of the insulin signaling pathway, including **(C)** mTOR^{S2448}, **(D)** GSK-3β^{S9}, and **(E)** Expression of GLUT4 was assessed in the *in vitro* model. The phosphorylated proteins are normalized to the non-phosphorylated protein levels, which in turn was normalized to β-tubulin or β-actin as internal loading controls. The effects of SMTNL1 vs. the empty vector-transfected cells were compared. **(F)** Relative glucose uptake was measured using 2-NBDG and the fluorescence values normalized to the protein concentration. Normalized values were compared to the empty vector-transfected cells treated with physiological levels of insulin InR: insulin resistant; MPA: medroxyprogesterone-17-acetate. (Two-way ANOVA and Sidak's *post hoc* test Mean ± SEM; n = 3; *, $p < 0.05$), and the effects of various treatments were also compared (Two-way ANOVA and Tukey's *post hoc* test Mean ± SEM; n = 3; $p < 0.05$; Different letters indicate significant differences between the groups compared). Fig. 4A and B were analyzed on the membrane after stripping.

Akt1 phosphorylation was significantly decreased in pregnant *Smtnl1* KO animals (Fig. S4D.).

To examine a wider range of Akt function in insulin signaling, the phosphorylation of two downstream Akt substrates was examined. Neither the expression level (Fig. S6A) nor the phosphorylation of mTOR at Ser2448 (Fig. 4C) was altered in the presence of chronic insulin administration or MPA exposure. However, when cells were co-treated with insulin and MPA, overexpression of FT-SMTNL1 activated mTOR. In addition, GSK-3β expression (Fig. S6C) and Ser9 phosphorylation levels (Fig. 4D) and p70S6 kinase phosphorylation at Thr389 (Fig. S5A) did not change, although p70S6 kinase protein expression showed InR-dependent elevation (Fig. S5B).

Finally, GLUT4 expression significantly increased in response to FT-SMTNL1 overexpression in InR cells compared to the transfection control (Fig. 4E). Moreover, glucose uptake was significantly elevated in SMTNL1-overexpressed myotubes compared to each of the vehicle control in insulin resistant samples, while it was decreased upon combined treatment of high glucose/high insulin and progesterone (Fig. 4F.). Collectively, these data demonstrate that FT-SMTNL1 overexpression promotes insulin signaling in myotubes by regulating the phosphorylation of several insulin-related downstream elements and leads elevated glucose uptake.

3.5. *SMTNL1 regulates JNK and ERK1/2 and IRS1 phosphorylation through expression of a novel PKC gene*

Next, we examined the potential upstream regulators of insulin signaling. Since both ERK1/2 and JNK were significantly altered in InR cells by Proteome Profiler analysis (Fig. 2.), we measured the expression and phosphorylation of these MAP kinases. JNK and ERK1/2 expressions were not modulated by any experimental condition (Fig. 5A and C). However, interestingly, the activating phosphorylation of JNK at Y185 and ERK1/2 at Thr202/Tyr204 increased significantly in response to 100 nM insulin treatment but was attenuated with FT-SMTNL1 overexpression in InR and MPA-treated C2C12 cells (Fig. 5B and D). We evaluated the target of SMTNL1 action on ERK1/2 and the upstream regulators of ERK1/2 activity. Protein phosphatase 2A expression did not change (Fig. 5E) but the levels of a novel protein kinase C, PKCε, were reduced by 50%

In response to FT-SMTNL1 overexpression compared to control

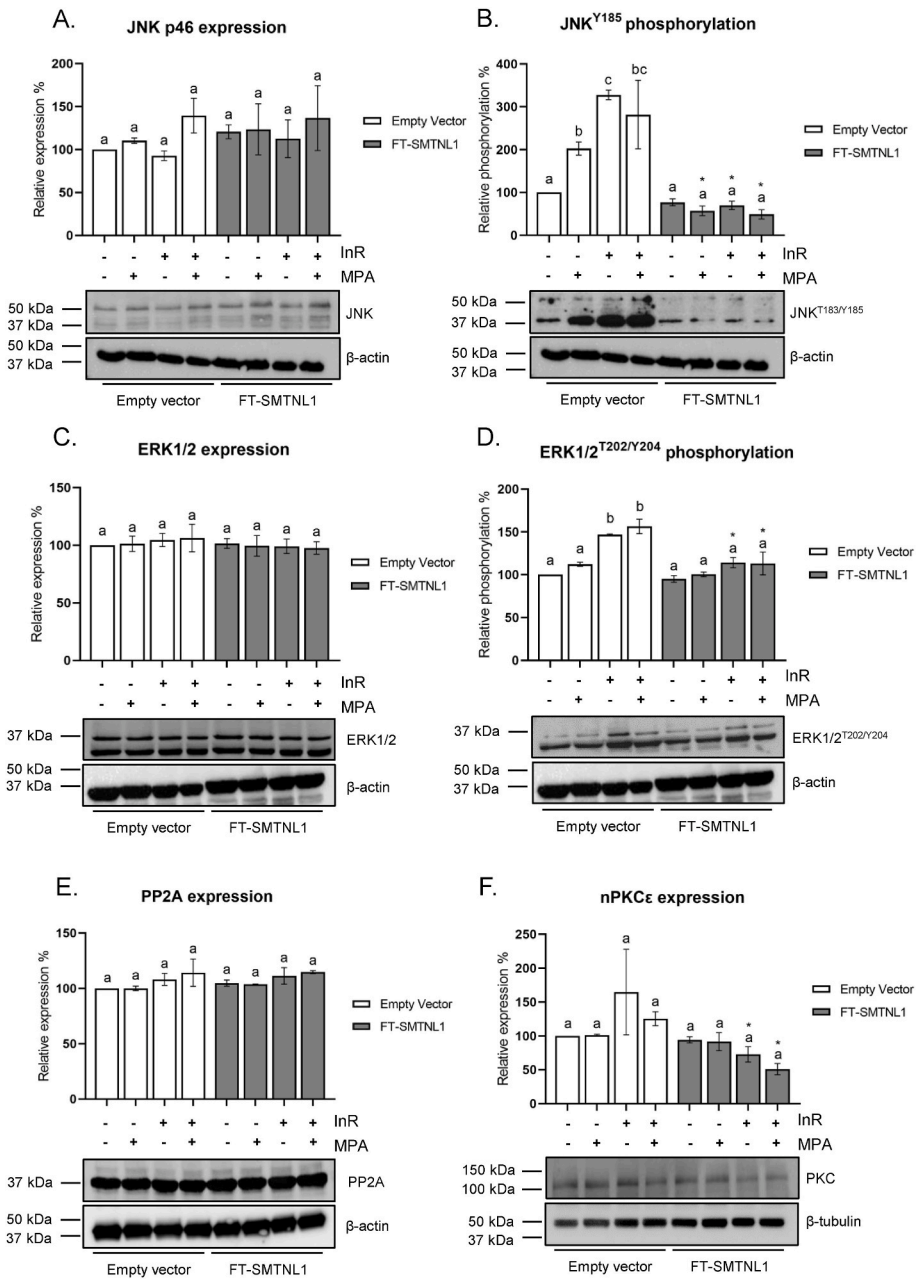

Fig. 5. Western blot analysis of JNK expression and phosphorylation, ERK1/2 expression and phosphorylation, and PP2A and PKC expression cells after induction of insulin resistance. Harvested samples were subjected to western blotting with **(A)** SAPK/JNK, **(B)** SAPK/JNK^{Y185}, **(C)** ERK1/2, **(D)** ERK1/2$^{T202/Y204}$, **(E)** PP2A, and **(F)** nPKCε antibodies. The phosphorylated proteins were normalized to the non-phosphorylated protein levels which in turn was normalized to β-actin as an internal loading control. InR: insulin resistant; MPA: medroxyprogesterone-17-acetate. The effect of SMTNL1 vs. the empty vector-transfected cells were compared (Two-way ANOVA and Sidak's *post hoc* test, Mean ± SEM; n = 3; *, $p < 0.05$), and the effects of various treatments were also compared (Two-way ANOVA and Tukey's *post hoc* test Mean ± SEM; n = 3; $p < 0.05$; Different letters indicate significant differences between the groups). Fig. 5A and B and 55C and D were analyzed on the membrane after stripping.

transfection in InR cells (Fig. 5F). Another potential regulator of IRS1 is atypical protein kinase C zeta (PKCζ), but no significant expression differences were detected for this kinase (Fig. S6D). These data indicate that SMTNL1 regulates ERK1/2 activity by reducing its upstream activator, PKCε.

3.6. *SMTNL1 improves glycolysis and mitochondrial respiration in insulin resistant myoblasts*

Changes in energy-producing pathways were determined using real-time, simultaneous measurements of oxygen consumption rate (OCR) and extracellular acidification rate (ECAR), as indicators of oxidative phosphorylation and glycolysis. We compared the effects of FT-SMTNL1 overexpression to empty vector controls in C2C12 cells after InR and MPA treatments. The conversion of glucose to lactate independent of oxygen releases protons into the extracellular medium and causes acidification that was measured as ECAR (Fig. 6A). Sequential injections of oligomycin and 2-DG combined with antimycin A measured glycolysis, glycolytic capacity, and allowed calculation of glycolytic reserve and non-glycolytic acidification. Baseline ECAR increased significantly in response to MPA treatment but drastically decreased in response to chronic insulin treatment. This reduction was ameliorated by FT-SMTNL1 overexpression in the presence of MPA (Fig. 6C). Similar tendencies were observed for anaerobic glycolytic values;

FT-SMTNL1 overexpression was associated with significant increase in ECAR only after treatment with MPA in InR when compared to cells transfected with the empty vector (Fig. 6E). Maximal glycolysis was increased by MPA and decreased in response to chronic insulin treatment but FT-SMTNL1 overexpression did not influence maximal glycolysis (Fig. 6G) nor the glycolytic reserve (Fig. S7A.).

Mitochondrial respiration was measured as OCR through chronological injection of etomoxir, oligomycin, FCCP, and antimycin A (Fig. 6B) to assess basal respiration, ATP production, proton leak, maximal respiration, and non-mitochondrial respiration. MPA increased

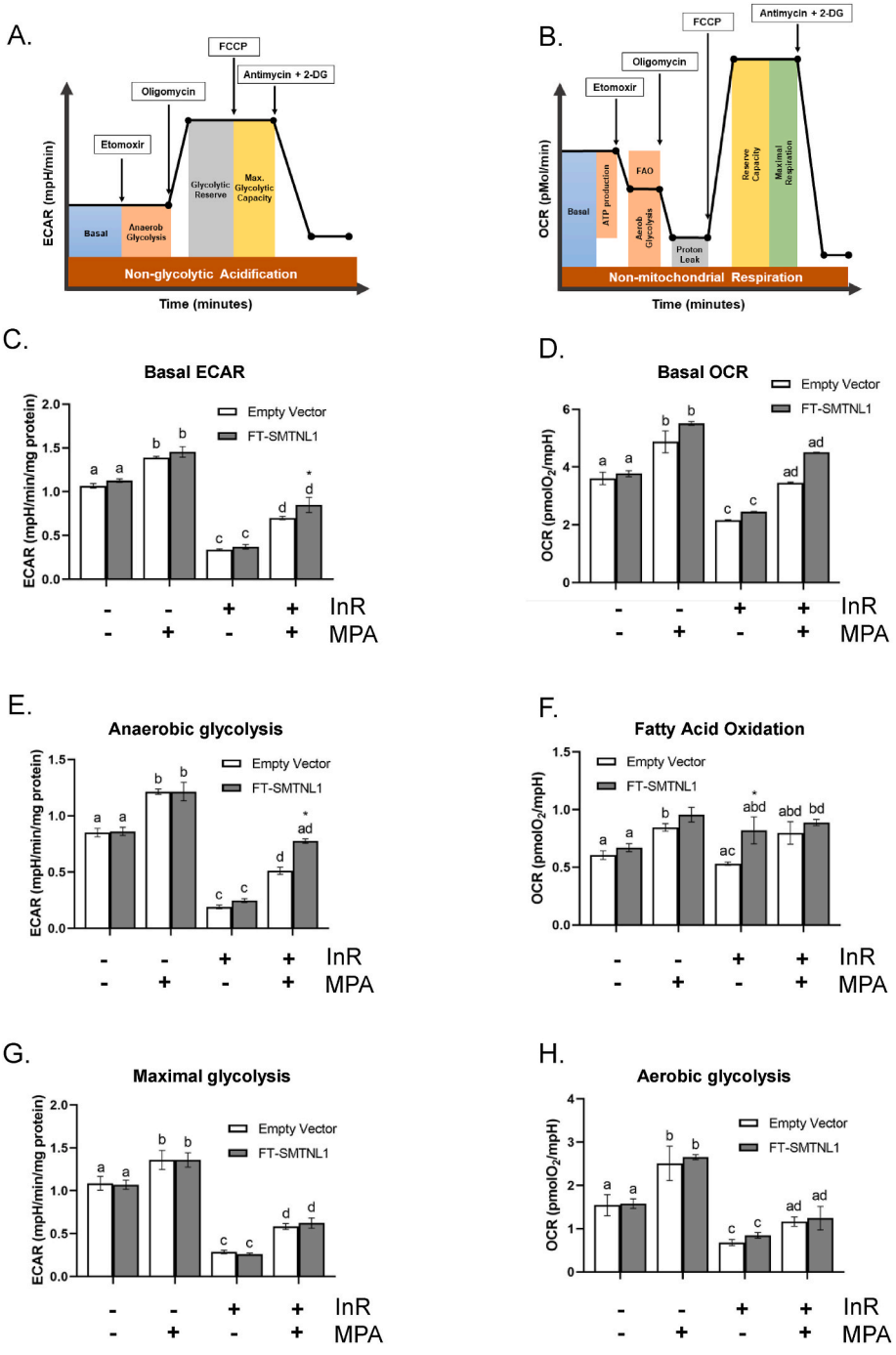

Fig. 6. Energetic parameters after transfection with SMTNL1 or empty vector in the C2C12 cell insulin resistance in vitro model. C2C12 cells were seeded on Seahorse XF 96, and cellular parameters were measured. Both glycolytic (ECAR – Extracellular Acidification Rate) and oxidative (OCR – Oxygen Consumption Rate) variables were measured. **(A–B)** Injection strategy used during the seahorse measurements. Before injecting the inhibitors, the baseline ECAR **(C)** and OCR **(D)** levels of the cells were measured. **(E)** Anaerobic glycolysis parameters independent of mitochondrial activity were calculated by subtracting the Antimycin A + 2-DG values from the baseline values. Fatty acid oxidation **(F)** was calculated by subtracting the OCR values measured after etomoxir injection from the baseline. **(G)** Maximal glycolysis was calculated by subtracting Antimycin A + 2-DG from values determined with oligomycin injection. **(H)** Aerobic glycolysis was calculated by subtracting the oligomycin injection values from the etomoxir injection; the difference is the glycolysis connected to mitochondrial activity. InR: insulin resistant; MPA: medroxyprogesterone-17-acetate. The effects of SMTNL1 vs. the empty vector-transfected cells were compared (Two-way ANOVA and Sidak's *post hoc* test, Mean ± SEM; n = 3; *, $p < 0.05$), and the effects of various treatments were compared (Two-way ANOVA and Tukey's *post hoc* test, Mean ± SEM; n = 3; $p < 0.05$; Different letters indicate that significant differences between the groups). The technical replicates were n = 23 per plate per treatment by dividing the 96 well plates into four regions (24–1) for the treatments and leaving one well for a blank in each region. After the measurements, values were normalized to protein content.

OCR in both control and InR cells. Chronic insulin exposure decreased basal OCR and MPA treatment prevented this reduction(Fig. 6D). The utilization of alternative carbon fuels, such as fatty acids was assessed as the difference between OCR values upon etomoxir and oligomycin treatments. MPA increased, InR decreased, and FT-SMTNL1 overexpression resulted in a slight elevation in fatty acid oxidation potential (Fig. 6F). Aerobic glycolysis (Fig. 6H), OCR reserve (Fig. S7B) and maximal respiration (Fig. S7C) were unaffected by the overexpression of SMTNL1. Collectively, these data imply that SMTNL1 predominantly acts on the glycolytic pathway where it significantly increased basal ECAR when compared to control cells. Taken together, the results confirm the insulin-sensitizing effects of SMTNL1 on the metabolism of InR cells.

4. Discussion

In the present study, we provide evidence for the metabolic role of SMTNL1 in differentiated C2C12 cells and a *Smtnl1* KO mouse model. In the presence of its natural ligand, progesterone, SMTNL1 overexpression was coupled to decreased Ser phosphorylation of IRS1, which induces the PI3K/Akt signaling pathway in C2C12 hyperinsulinemic/hypoglycemic insulin-resistant myotubes. Our data indicate that SMTNL1 exerts its effects by regulating the expression of a novel PKC that contributes to the phosphorylation of IRS1 directly at Ser318 residue and indirectly at Ser612 through the regulation of ERK1/2.

Insulin signaling and the related signal transduction cascades involved in insulin resistance in SKM pathology were previously investigated by comprehensive mass spectrometry-based proteomic analysis

(Mullen and Ohlendieck, 2010). In addition, numerous studies have revealed the phosphorylation-level changes of players in insulin signaling showing the importance of this field. We prescreened the possible signaling pathways altered by SMTNL1 with InR of C2C12 myotubes using a series of proteome profiler assays. To differentiate between the cytoskeletal and transcriptional effects of SMTNL1, experiments were completed with progesterone as the natural ligand of SMTNL1. We narrowed down the SMTNL1-related pathways primarily to mTOR and Ser/Thr kinase signaling (Fig. 1). These results are broadly in line with an earlier report of *Smtnl1* KO mice using proteomic and microarray analyses (Lontay et al., 2015).

Our results indicate that IRS1 phosphorylation at Ser307, Ser318, and Ser612 was upregulated in the InR model and SMTNL1 overexpression decreased phosphorylation at these residues but only in the presence of progesterone. Under InR conditions, the shift from Tyr to Ser phosphorylation of IRS1 leads to the dissociation of IRS1 from PI3K, which accounts for insulin signaling defects (Morino et al., 2006). IRS1 Ser307 and Ser318 phosphorylation disrupts the IR/IRS1 complex and enables desensitization to insulin (Copps and White, 2012). Ser307 is the major site on IRS1 for JNK phosphorylation (Mussig et al., 2005) our results were in accordance with other *in vivo* diabetic animal and *in vitro* studies (Manning and Davis, 2003) showing that JNK activity was upregulated in InR cells. Over-expression of SMTNL1 did not change the expression of JNK, but their activation were significantly suppressed in response to SMTNL1 overexpression in InR model. We also characterized IRS1 Ser318 phosphorylation, which is the target of insulin-induced PKCζ (Moeschel et al., 2004); however, the activity and expression of this PKC isoform were not SMTNL1-dependent. Deletion of any member of the novel PKC family prevents InR by decreasing IRS1 phosphorylation on Ser308 and Ser318 (Boucher et al., 2014); we showed that Ser318 phosphorylation was attenuated by SMTNL1 overexpression with coincident downregulation of novel PKCε levels.

The phosphorylation of the Ser612 residue of IRS1, located proximal to the regulatory Tyr residues, provides negative regulation of the insulin signaling pathway involving predominantly ERK1/2 and the mTOR pathways in its regulation. ERK1/2 activation plays a major role in maintaining insulin-induced PI3K-dependent InR (Gual et al., 2003) and specific inhibition of ERK1/2 by PD98059 restored insulin sensitivity (Fujishiro et al., 2003). In our model, ERK1/2 was phosphorylated after chronic insulin treatment and overexpression of SMTNL1 suppressed ERK1/2 activity, especially in the presence of MPA. In addition, IRS1 Ser612 phosphorylation was reduced, likely resultant of the SMTNL1-dependent reduction of ERK1/2 activity. We suggest that ERK1/2 exerts insulin-desensitizing effect in C2C12 myotubes not only through the phosphorylation of Ser612 but also through the regulation of GLUT4 since chronic activation of ERK1/2 leads to the downregulation of GLUT4 expression and decreased insulin-induced glucose transport (Krook et al., 2000).

JNK and ERK1/2 protein expression did not change but their phosphorylation and, presumably, activity decreased in response to SMTNL1 overexpression with progesterone, suggesting that SMTNL1 regulates upstream Ser/Thr kinases or phosphatases at the gene expression level. None of the MAP kinase kinases were altered in the microarray analysis of pregnant *Smtnl1* KO mice compared to WT (Lontay et al., 2015). Therefore, we investigated protein phosphatase 2A (PP2A), the negative regulator of ERK1/2 (Yu et al., 2004) but its gene expression was unaffected in this study (Fig. 5E). Another potential regulator is the novel PKCε that phosphorylates and activates ERK1/2 in SKM. In our study, PKCε expression was downregulated by SMTNL1 in the InR C2C12 cells, promoting insulin sensitivity through several mechanisms. In diabetic rats, PKCε was prominently overexpressed in the SKM and hyperinsulinemia leading to insulin resistance in SKM was associated with chronic activation of PKCε but not other novel PKC isoforms (Ikeda et al., 2001). It is in line with previous findings showing an alteration in PKC isoforms in SMTNL1 KO animals by microarray analysis (Lontay et al., 2015). We suggest that JNK activity is regulated by its upstream regulator, dual specific phosphatase 9 (Major et al., 2021) that was identified as an SMTNL1-dependent gene in SKM in mice (Lontay et al., 2015).

The mTORC1/S6K1 pathway provides a negative feedback loop to attenuate PI3K/Akt signaling downstream of IRS1 via the phosphorylation of Ser1101 in SKM (Kido et al., 2020). Strikingly, our results showed a significant decrease in IRS1 Ser1101 phosphorylation with InR, which was further suppressed with overexpression of SMTNL1. Consistent with this finding, phosphorylation of IRS1 Ser1101 was elevated in pregnant *Smtnl1* KO animals but not pregnant WT animals. No other studies have monitored the effects of long-term hyperinsulinemia on Ser1101 phosphorylation in differentiated C2C12 cells. We presume that these results are due to the long-term InR state of myotubes and the activation of inhibitory regulatory feedback signals for the phosphorylation of the Ser1101 residue. IRS1 degradation also contributes to the downregulation of insulin-induced signaling, as revealed in our InR model in a SMTNL1-independent manner and in the literature (Pederson et al., 2001).

PI3K activity, measured by the concentration of liberated PIP_3 (Fig. 3), was increased upon insulin stimulation of C2C12 myotubes but this level was significantly lower in cells with InR. The expression of p85 expression decreased in InR cells, but SMTNL1 overexpression restored p85 expression and PI3K activity in the presence of MPA. Alteration in PI3K also affects the activity of its downstream effector, Akt. Interestingly, the protein levels of Akt1 did not change in response to any treatments in differentiated C2C12 cells similarly to the findings in human diabetic SKM samples (Czech and Corvera, 1999). Based on our results, SMTNL1 differentially regulated Ser473 and Thr308 phosphorylation of Akt (Fig. 4A and B). Insulin-induced Akt phosphorylation at both Thr308 and Ser473 was significantly decreased in InR non-transfected cells. However, SMTNL1 overexpression elevated Thr308 phosphorylation in insulin-induced control cells but only slightly induced Ser473 phosphorylation in InR cells compared to the control. For insulin-induced activation, Akt requires the hierarchical phosphorylation of both Thr308 and Ser473 phosphorylated by phosphoinositide-dependent kinase-1 (PDK1) and mTORC2, respectively (Copps and White, 2012). Chronic insulin exposure inhibits Akt activation via inhibition of Akt Thr308 phosphorylation, even without changes in Akt Ser473 phosphorylation (Kondapaka et al., 2004). These results indicate that Akt Ser473 does not fully reflect upstream IRS1/PI3K signaling.

Akt also phosphorylates and inactivates its downstream substrate, GSK-3β, resulting in glycogen synthase activation and glycogen accumulation (Kim et al., 2004). Surprisingly, the phosphorylation of GSK-3β was unaffected under every experimental condition. Similarly, *Shao* et al. showed no change in GSK3β phosphorylation in the muscle after insulin treatment in *db/db* mice even with a twofold increase in Akt Ser473 phosphorylation (Shao et al., 2000) and the phosphorylation of downstream Akt substrates Akt substrate of 160 kDa was also unaffected (Karlsson et al., 2006). Based on our proteome profiler analysis, eNOS, PRAS40, and WNK1, which are classic substrates of PI3K/Akt, were phosphorylated by Akt activation. These combined results suggest that SMTNL1 selectively regulates impaired Akt activity related to insulin resistance and may be responsible for the heterogeneous downstream effects of Akt (Gonzalez et al., 2011; Li et al., 2010).

The PI3K/Akt pathway regulates downstream signaling in the mTOR pathway to coordinate cell growth and modulate the nutrient response. Akt phosphorylates mTOR at Thr2446/Ser2448 (Sekulic et al., 2000); this residue can also be phosphorylated by p70S6 kinase (p70S6K) (Chiang and Abraham, 2005). Our results are in line with these findings. Changes in Akt1 Ser473 mirrored that of mTOR and increased in InR and insulin-induced cells in response to SMTNL1. These data demonstrate that the PI3K-Akt-mTOR pathway is regulated by SMTNL1, without modulating the expression and activity of p70S6K. Another downstream target of insulin/PI3K signaling is Glut4, which is translocated to the plasma membrane, leading to increased glucose transport *in vitro* (Czech

and Corvera, 1999; Shepherd et al., 1998). Overexpression of SMTNL1 in C2C12 myotubes was associated with enhanced GLUT4 expression in InR (Fig. 4F). Enhanced GLUT4 expression in muscle tissue reduces blood glucose. In agreement with these findings, skeletal muscle GLUT4 expression was significantly lower in *Smtnl1*−/− mice (Lontay et al., 2015).

Glycolytic function and mitochondrial respiration also demonstrated the insulin-sensitizing effects of SMTNL1 on InR C2C12 cells. Base ECAR and anaerobic glycolysis were decreased in InR cells. However, SMTNL1 overexpression in the presence of progesterone attenuated the decreased ECAR and glycolysis without affecting either maximal glycolysis or glycolytic reserve capacity. Progesterone increased glycolytic activity and ATP production in skeletal muscle cells but the activities were still below control levels in InR cells; only SMTNL1 overexpression in the presence of progesterone could rescue glycolytic activity and ATP production. In agreement with these results, *smtnl1* KO mice were metabolically less efficient and showed glucose intolerance; pregnancy increased glucose tolerance to the level of WT animals (Lontay et al., 2015), confirming the regulatory effects of SMTNL1 on gene expression in the insulin signaling pathway. The rate of fatty acid uptake was higher and the rate of fatty acid oxidation was lower in insulin-resistant muscle cells compared to healthy cells (Turcotte and Fisher, 2008), which was confirmed in our cell culture model. Interestingly, SMTNL1 induced fatty acid oxidation in InR cells. This is in line with data in *smtnl1* KO pregnant animals, in which skeletal muscle glycolysis and fatty acid oxidation were decreased (Lontay et al., 2015).

Our data might have implications in gestational diabetes mellitus (GDM). GDM is characterized by severe insulin resistance and an increased risk of developing subsequent type 2 diabetes. MPA is a co-regulator in this study, but also serves as a model for GDM, where glucose, insulin, and progesterone levels are elevated. In patients with GDM, the maximal insulin-stimulated IRS1 Tyr phosphorylation was significantly lower compared with non-pregnant control subjects and glucose transport activity was reduced (Friedman et al., 1999). Furthermore, redistribution of PI3K to the IR was impaired due to increased insulin-stimulated IRS1 Ser-phosphorylation and PI3K activity was reduced with hampered GLUT4 translocation in GDM patients (Shao et al., 2002). *Smtnl1* KO animals developed insulin resistance, which was significantly worsened in pregnancy (Lontay et al., 2015). The promotion of Ser phosphorylation on residues Ser307, Ser612 and Ser318 of IRS1 with SMTNL1 overexpression was dependent on progesterone and correlated with PI3K activity. These results indicate that SMTNL1 regulation of gene expression can prevent GDM.

5. Conclusions

These data collectively suggest that SMTNL1 induces insulin-sensitization of C2C12 myotubes through several mechanisms. 1) SMTNL1 negatively regulates the expression of the upstream regulators of insulin-dependent Ser/Thr kinases that are activated by prolonged insulin and glucose exposure. By decreasing PKCε expression, SMTNL1 hampers the activity of ERK1/2 with subsequent decrease in IRS1 Ser612 phosphorylation and initiation of PI3K association to activate the PI3K-Akt-mTOR pathway. 2) SMTNL1 also acts on heterologous IRS1 kinases to inhibit insulin action during the development of insulin resistance by regulating IRS1 Ser307 phosphorylation that in turn would affect IR/IRS1 interactions. 3) SMTNL1 promotes glucose uptake via activation of Akt pathways and by inducing GLUT4 expression to overcome insulin resistance (Fig. 7). Taken together, these findings indicate that SMTNL1 serves as an important regulator of insulin

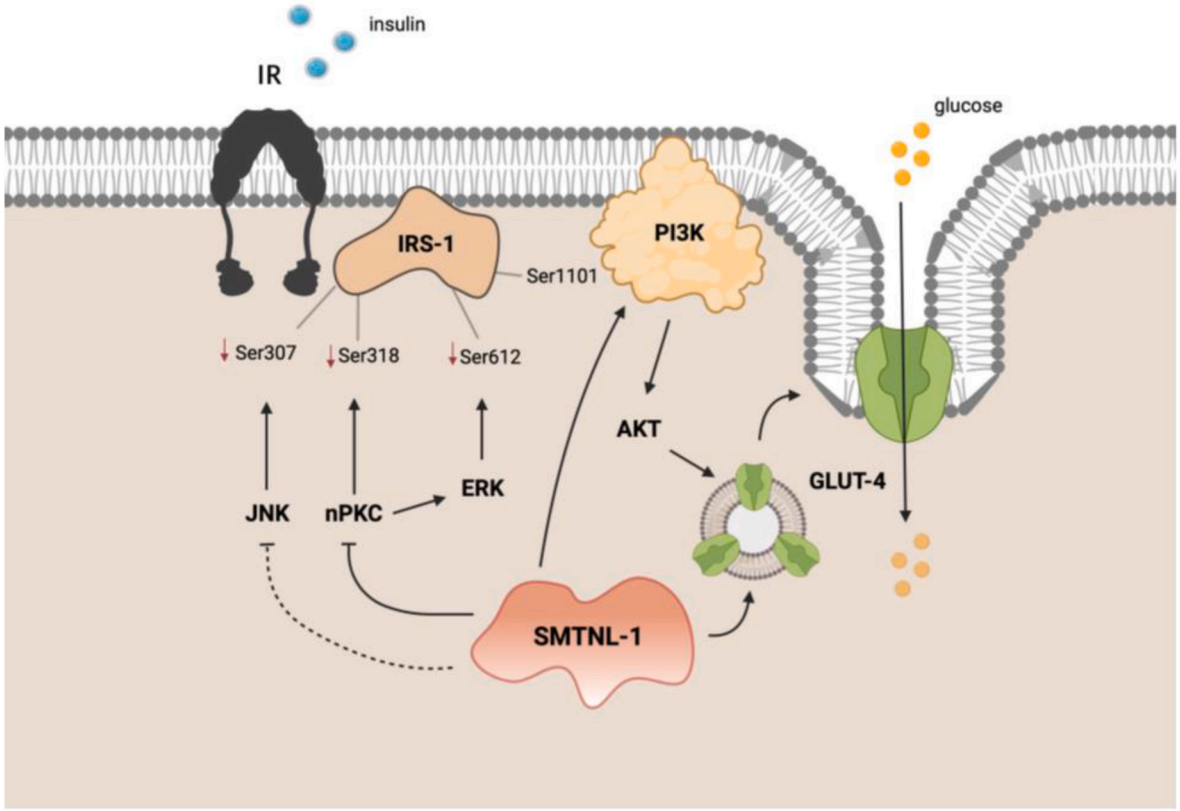

Fig. 7. Insulin sensitizing effects of SMTNL1 in InR C2C12 myotubes. SMTNL1 decreased PKCε gene expression, which hampered the activity of ERK1/2 leading to a decrease in IRS1 Ser612 phosphorylation. Ser612 phosphorylation initiates the PI3K association, activates the PI3K-Akt-mTOR pathway, and downregulates JNK activation, leading to a decreased IRS1 Ser307 phosphorylation. SMTNL1 promotes glucose uptake via activation of Akt and AMPK pathways and by inducing GLUT4 expression.

signaling in SKM. Thus, SMTNL1 is a potential therapeutic target for improving insulin resistance.

6. Funding information

This work was supported by grants from the National Research, Development and Innovation Office (FK125043), the University of Debrecen, Faculty of Medicine Research Fund (1G3DBKJ0BFTK 247) for B. L, and from the EU co-financed by the European Regional Development Fund under project EFOP-3.6.2-16-2017-00006 and EFOP-3.6.3-VEKOP-16-2017-00009.

8. Conflicts of interest

The authors have declared no competing interests.

CRediT authorship contribution statement

Istvan Tamas: Writing – review & editing, completed Fig. 1, 2 and 3Fig. 1fig2fig3, wrote the paper. All authors reviewed the manuscript. **Evelin Major:** performed Fig S2 and assisted in Fig. 6. **Daniel Horvath:** completed Fig. 5A-Bfig5, 4E-F. **Ilka Keller:** created Fig. 7. **Adam Ungvari:** completed Fig. 5A–B, 4E-F. **Timothy A. Haystead:** Writing – review & editing, wrote the paper. All authors reviewed the manuscript. **Justin A. MacDonald:** supported animal experiments. **Beata Lontay:** Writing – review & editing, designed the study, wrote the paper. All authors reviewed the manuscript.

9. Acknowledgements

We thank Dr Karen Uray for providing language help and Andrea Docsa and Ágota Kelemenné Szántó for technical assistance.

Appendix A. Supplementary data

Supplementary data to this article can be found online at https://doi.org/10.1016/j.mce.2022.111663.

References

Abdul-Ghani, M.A., DeFronzo, R.A., 2009. Plasma glucose concentration and prediction of future risk of type 2 diabetes. Diabetes Care 32 (Suppl. 2), S194–S198.
Beg, M., Abdullah, N., Thowfeik, F.S., Altorki, N.K., McGraw, T.E., 2017. Distinct Akt phosphorylation states are required for insulin regulated Glut4 and Glut1-mediated glucose uptake. Elife 6.
Bodoor, K., Lontay, B., Safi, R., Weitzel, D.H., Loiselle, D., Wei, Z., Lengyel, S., McDonnell, D.P., Haystead, T.A., 2011. Smoothelin-like 1 protein is a bifunctional regulator of the progesterone receptor during pregnancy. J. Biol. Chem. 286, 31839–31851.
Borman, M.A., MacDonald, J.A., Haystead, T.A., 2004. Modulation of smooth muscle contractility by CHASM, a novel member of the smoothelin family of proteins. FEBS Lett. 573, 207–213.
Boucher, J., Kleinridders, A., Kahn, C.R., 2014. Insulin receptor signaling in normal and insulin-resistant states. Cold Spring Harbor Perspect. Biol. 6.
Chiang, G.G., Abraham, R.T., 2005. Phosphorylation of mammalian target of rapamycin (mTOR) at Ser-2448 is mediated by p70S6 kinase. J. Biol. Chem. 280, 25485–25490.
Copps, K.D., White, M.F., 2012. Regulation of insulin sensitivity by serine/threonine phosphorylation of insulin receptor substrate proteins IRS1 and IRS2. Diabetologia 55, 2565–2582.
Czech, M.P., Corvera, S., 1999. Signaling mechanisms that regulate glucose transport. J. Biol. Chem. 274, 1865–1868.
Friedman, J.E., Ishizuka, T., Shao, J., Huston, L., Highman, T., Catalano, P., 1999. Impaired glucose transport and insulin receptor tyrosine phosphorylation in skeletal muscle from obese women with gestational diabetes. Diabetes 48, 1807–1814.
Fujishiro, M., Gotoh, Y., Katagiri, H., Sakoda, H., Ogihara, T., Anai, M., Onishi, Y., Ono, H., Abe, M., Shojima, N., et al., 2003. Three mitogen-activated protein kinases inhibit insulin signaling by different mechanisms in 3T3-L1 adipocytes. Mol. Endocrinol. 17, 487–497.
Gonzalez, E., Flier, E., Molle, D., Accili, D., McGraw, T.E., 2011. Hyperinsulinemia leads to uncoupled insulin regulation of the GLUT4 glucose transporter and the FoxO1 transcription factor. Proc. Natl. Acad. Sci. U. S. A. 108, 10162–10167.
Gual, P., Gremeaux, T., Gonzalez, T., Le Marchand-Brustel, Y., Tanti, J.F., 2003. MAP kinases and mTOR mediate insulin-induced phosphorylation of insulin receptor substrate-1 on serine residues 307, 612 and 632. Diabetologia 46, 1532–1542.
Ikeda, Y., Olsen, G.S., Ziv, E., Hansen, L.L., Busch, A.K., Hansen, B.F., Shafrir, E., Mosthaf-Seedorf, L., 2001. Cellular mechanism of nutritionally induced insulin resistance in Psammomys obesus: overexpression of protein kinase Cepsilon in skeletal muscle precedes the onset of hyperinsulinemia and hyperglycemia. Diabetes 50, 584–592.
Karlsson, H.K., Ahlsen, M., Zierath, J.R., Wallberg-Henriksson, H., Koistinen, H.A., 2006. Insulin signaling and glucose transport in skeletal muscle from first-degree relatives of type 2 diabetic patients. Diabetes 55, 1283–1288.
Kido, K., Sase, K., Yokokawa, T., Fujita, S., 2020. Enhanced skeletal muscle insulin sensitivity after acute resistance-type exercise is upregulated by rapamycin-sensitive mTOR complex 1 inhibition. Sci. Rep. 10, 8509.
Kim, K.H., Song, M.J., Yoo, E.J., Choe, S.S., Park, S.D., Kim, J.B., 2004. Regulatory role of glycogen synthase kinase 3 for transcriptional activity of ADD1/SREBP1c. J. Biol. Chem. 279, 51999–52006.
Kohn, A.D., Summers, S.A., Birnbaum, M.J., Roth, R.A., 1996. Expression of a constitutively active Akt Ser/Thr kinase in 3T3-L1 adipocytes stimulates glucose uptake and glucose transporter 4 translocation. J. Biol. Chem. 271, 31372–31378.
Kondapaka, S.B., Zarnowski, M., Yver, D.R., Sausville, E.A., Cushman, S.W., 2004. 7-hydroxystaurosporine (UCN-01) inhibition of Akt Thr308 but not Ser473 phosphorylation: a basis for decreased insulin-stimulated glucose transport. Clin. Cancer Res. 10, 7192–7198.
Krook, A., Bjornholm, M., Galuska, D., Jiang, X.J., Fahlman, R., Myers Jr., M.G., Wallberg-Henriksson, H., Zierath, J.R., 2000. Characterization of signal transduction and glucose transport in skeletal muscle from type 2 diabetic patients. Diabetes 49, 284–292.
Kupriyanova, T.A., Kandror, K.V., 1999. Akt-2 binds to Glut4-containing vesicles and phosphorylates their component proteins in response to insulin. J. Biol. Chem. 274, 1458–1464.
Li, S., Brown, M.S., Goldstein, J.L., 2010. Bifurcation of insulin signaling pathway in rat liver: mTORC1 required for stimulation of lipogenesis, but not inhibition of gluconeogenesis. Proc. Natl. Acad. Sci. U. S. A. 107, 3441–3446.
Lontay, B., Bodoor, K., Sipos, A., Weitzel, D.H., Loiselle, D., Safi, R., Zheng, D., Devente, J., Hickner, R.C., McDonnell, D.P., et al., 2015. Pregnancy and smoothelin-like protein 1 (SMTNL1) deletion promote the switching of skeletal muscle to a glycolytic phenotype in human and mice. J. Biol. Chem. 290, 17985–17998.
Lontay, B., Bodoor, K., Weitzel, D.H., Loiselle, D., Fortner, C., Lengyel, S., Zheng, D., Devente, J., Hickner, R., Haystead, T.A., 2010. Smoothelin-like 1 protein regulates myosin phosphatase-targeting subunit 1 expression during sexual development and pregnancy. J. Biol. Chem. 285, 29357–29366.
Major, E., Gyory, F., Horvath, D., Keller, I., Tamas, I., Uray, K., Fulop, P., Lontay, B., 2021. Smoothelin-like protein 1 regulates development and metabolic transformation of skeletal muscle in hyperthyroidism. Front. Endocrinol. 12, 751488.
Manning, A.M., Davis, R.J., 2003. Targeting JNK for therapeutic benefit: from junk to gold? Nat. Rev. Drug Discov. 2, 554–565.
Mathe, C., Beyer, D., Erdodi, F., Serfozo, Z., Szekvolgyi, L., Vasas, G.M.M.H., Jambrik, K., Gonda, S., Kiss, A., et al., 2009. Microcystin-LR induces abnormal root development by altering microtubule organization in tissue-cultured common reed (Phragmites australis) plantlets. Aquat. Toxicol. 92, 122–130.
Meigs, J.B., 2003. Epidemiology of the insulin resistance syndrome. Curr. Diabetes Rep. 3, 73–79.
Mlinar, B., Marc, J., Janez, A., Pfeifer, M., 2007. Molecular mechanisms of insulin resistance and associated diseases. Clin. Chim. Acta 375, 20–35.
Moeschel, K., Beck, A., Weigert, C., Lammers, R., Kalbacher, H., Voelter, W., Schleicher, E.D., Haring, H.U., Lehmann, R., 2004. Protein kinase C-zeta-induced phosphorylation of Ser318 in insulin receptor substrate-1 (IRS-1) attenuates the interaction with the insulin receptor and the tyrosine phosphorylation of IRS-1. J. Biol. Chem. 279, 25157–25163.
Morino, K., Petersen, K.F., Shulman, G.I., 2006. Molecular mechanisms of insulin resistance in humans and their potential links with mitochondrial dysfunction. Diabetes 55 (Suppl. 2), S9–S15.
Mullen, E., Ohlendieck, K., 2010. Proteomic profiling of non-obese type 2 diabetic skeletal muscle. Int. J. Mol. Med. 25, 445–458.
Mussig, K., Fiedler, H., Staiger, H., Weigert, C., Lehmann, R., Schleicher, E.D., Haring, H. U., 2005. Insulin-induced stimulation of JNK and the PI 3-kinase/mTOR pathway leads to phosphorylation of serine 318 of IRS-1 in C2C12 myotubes. Biochem. Biophys. Res. Commun. 335, 819–825.
Pederson, T.M., Kramer, D.L., Rondinone, C.M., 2001. Serine/threonine phosphorylation of IRS-1 triggers its degradation: possible regulation by tyrosine phosphorylation. Diabetes 50, 24–31.
Sekulic, A., Hudson, C.C., Homme, J.L., Yin, P., Otterness, D.M., Karnitz, L.M., Abraham, R.T., 2000. A direct linkage between the phosphoinositide 3-kinase-AKT signaling pathway and the mammalian target of rapamycin in mitogen-stimulated and transformed cells. Cancer Res. 60, 3504–3513.
Shao, J., Yamashita, H., Qiao, L., Draznin, B., Friedman, J.E., 2002. Phosphatidylinositol 3-kinase redistribution is associated with skeletal muscle insulin resistance in gestational diabetes mellitus. Diabetes 51, 19–29.
Shao, J., Yamashita, H., Qiao, L., Friedman, J.E., 2000. Decreased Akt kinase activity and insulin resistance in C57BL/KsJ-Leprdb/db mice. J. Endocrinol. 167, 107–115.
Shepherd, P.R., Withers, D.J., Siddle, K., 1998. Phosphoinositide 3-kinase: the key switch mechanism in insulin signalling. Biochem. J. 333 (Pt 3), 471–490.
Sipos, A., Ivan, J., Becsi, B., Darula, Z., Tamas, I., Horvath, D., Medzihradszky, K.F., Erdodi, F., Lontay, B., 2017. Myosin phosphatase and RhoA-activated kinase modulate arginine methylation by the regulation of protein arginine methyltransferase 5 in hepatocellular carcinoma cells. Sci. Rep. 7, 40590.

Turcotte, L.P., Fisher, J.S., 2008. Skeletal muscle insulin resistance: roles of fatty acid metabolism and exercise. Phys. Ther. 88, 1279–1296.
Wong, C.Y., Al-Salami, H., Dass, C.R., 2020. C2C12 cell model: its role in understanding of insulin resistance at the molecular level and pharmaceutical development at the preclinical stage. J. Pharm. Pharmacol. 72, 1667–1693.
Wooldridge, A.A., Fortner, C.N., Lontay, B., Akimoto, T., Neppl, R.L., Facemire, C., Datto, M.B., Kwon, A., McCook, E., Li, P., et al., 2008. Deletion of the protein kinase A/protein kinase G target SMTNL1 promotes an exercise-adapted phenotype in vascular smooth muscle. J. Biol. Chem. 283, 11850–11859.
Yu, L.G., Packman, L.C., Weldon, M., Hamlett, J., Rhodes, J.M., 2004. Protein phosphatase 2A, a negative regulator of the ERK signaling pathway, is activated by tyrosine phosphorylation of putative HLA class II-associated protein I (PHAPI)/pp32 in response to the antiproliferative lectin, jacalin. J. Biol. Chem. 279, 41377–41383.